

RESEARCH PAPER



MicroRNA-138 improves LPS-induced trophoblast dysfunction through targeting RELA and NF- κ B signaling

Ailan Yin, Qian Chen, Mei Zhong, and Bei Jia

Department of Gynecology and Obstetrics, Nanfang Hospital, Southern Medical University, Guangzhou, China

ABSTRACT

Preeclampsia is a pregnancy complication classified by new onset of elevated blood pressure and proteinuria after 20 weeks of gestation. During preeclampsia, extra villous trophoblasts fail to adequately invade the myometrial spiral arteries, leading to incomplete and impaired vessel transformation and initiating or aggravating preeclampsia. Although NF- κ B and proinflammatory cytokines have been reported to be related to trophoblast dysfunction, the underlying mechanism remains unclear. Herein, we demonstrated the miR-138/RELA axis modulating the migratory ability, and invasive ability of HTR-8/SVneo and JEG-3 cells, as well as the inflammatory factor levels in response to LPS stimulation. miR-138 expression was upregulated in preeclampsia placenta and LPS-stimulated HTR-8/SVneo and JEG-3 cell lines. miR-138 overexpression rescued the migratory and invasive ability of HTR-8/SVneo and JEG-3 cells inhibited by LPS stimulation, and decreased LPS-induced TNF- α and IL-6 levels. By binding the 3'-UTR of RELA, miR-138 negatively regulated p65 expression. The silencing of p65 also improved LPS-induced HTR-8/SVneo and JEG-3 cell dysfunction and TNF- α and IL-6 levels. More importantly, p65 overexpression partially reversed the functions of miR-138 overexpression upon both cells, indicating that miR-138 exerted its biological effects through targeting RELA. In conclusion, miR-138 improves LPS-induced inflammation and oxidative stress on trophoblasts through targeting RELA and affecting NF- κ B signaling. The miR-138/RELA axis might be involved in preeclampsia pathogenesis, which requires further *in vivo* and clinical researches.

ARTICLE HISTORY

Received 29 September 2020
Revised 17 December 2020
Accepted 13 January 2021

KEYWORDS

Preeclampsia (PE);
inflammation; miR-138; p65
(RELA); trophoblast

Introduction


Preeclampsia, a pregnancy complication, is a condition classified by new onset of elevated blood pressure and proteinuria after 20 weeks of gestation. Although preeclamptic pathogenesis remains unclear, it has been reported to be related to inflammation, oxidative stress, and extra villous trophoblast and endothelial dysfunction [1–3].

In the early stages of normal placental development, extra villous cytotrophoblasts invade the uterine spiral arteries of the decidua and myometrium, replacing uterine vessel endothelial layer and transforming these small resistance vessels to flaccid, high-caliber capacitance vessels. Subsequently, the uterine blood flow required for sustaining the fetus through the pregnancy is, thus, increased [4]. However, in preeclampsia, the described vessel transformation is incomplete and impaired [5]. Due to increased cell apoptosis [6], decreased cell proliferation [7], and altered cell migration and invasion [8],

extra villous trophoblasts will fail to adequately invade the myometrial spiral arteries. Thus, further investigating the molecular mechanisms of trophoblast dysregulation, in particularly invasion and migration, would be of great value for preeclampsia treatment.

Within preeclamptic patients, the circulating levels of pro-inflammatory cytokines, such as TNF- α (tumor necrosis factor alpha), show to be increased within maternal and cord blood [9], resulting in an increase in reactive oxygen species (ROS)-induced oxidative stress [10] and endothelium dysfunction [11], leading to the progression of high blood pressure and proteinuria [12]. Within a trophoblast-like cell line, oxidative stress activates the transcription factor NF- κ B (nuclear factor-kappa B) and TNF- α enhances NF- κ B activation [13], whose activation shows to be dramatically promoted within the placentas of preeclampsia than that within normal placentas [13]. In turn, NF- κ B

CONTACT Bei Jia  jiabei@smu.edu.cn

 Supplemental data for this article can be accessed [here](#).

© 2021 Informa UK Limited, trading as Taylor & Francis Group

and TNF- α form a positive feedback loop, progressively worsening inflammation in the placenta [13]. Moreover, several pharmacological studies indicate that the protection of aspirin against TNF- α -caused endothelium dysfunction [14] and LPS-induced preeclampsia-like syndromes in mice [15] through inhibiting NF- κ B signaling pathway. Thus, searching for effective ways of downregulating the levels of NF- κ B and proinflammatory cytokines might be promising strategy for improving trophoblast dysfunction and preeclampsia.

miRNA is one of the most important classes of tissue-specific gene expression regulators. Via interacting with target mRNAs in their 3'-UTR, miRNAs could induce the degradation or transcription inhibition of target mRNAs, depending on the complementary [16,17]. In preeclampsia, increasing evidence indicate that a great amount of miRNAs show to be deregulated in preeclampsia placentas compared with normal placentas [18–20]. LPS or TNF- α stimulation also leads to the changes in the expression levels of various miRNAs, including miR-146a, miR-21, and miR-155 [21–23]. Deregulated miRNAs are involved in preeclampsia pathogenesis through a variety of mechanisms. For example, miR-155 expression showed to be elevated together with NF- κ B in HTR-8/SVneo, a human-trophoblast-derived cell line stimulated with low dose of LPS, and was involved in the remodeling of HTR-8/SVneo cells induced by LPS [24]. Within TNF- α -treated human endothelium, TNF- α -mediated inducible effects of miR-31-5p were blocked via an NF- κ B inhibitor and NF- κ B p65 silencing; TNF- α and miR-31-5p mimic induced endothelium dysfunction, leading to angiogenic defects, trophoblast invasiveness, and vascular relaxation in an *ex vivo* cultured human placental artery models, which are considered as typical preeclamptic characteristics [25]. Thus, miRNAs that target NF- κ B p65 might be potential agent for improving inflammation-related endothelial dysfunction during preeclampsia.

In the present study, we analyzed the different expressed miRNAs in preeclampsia related microarray GSE96983 and GSE103542. We found that miR-138-5p were significantly downregulated in preeclampsia placenta tissues and late preeclampsia placenta tissues. Thus, miR-138 was selected for further

experiments. The specific effects of miR-138 on trophoblast functions, including migration, invasion, and inflammatory factor levels were examined. The predicted binding between miR-138 and RELA, as well as miR-138 negative regulation of RELA were examined. The specific effects of p65 on trophoblast functions and inflammatory factor levels were also detected. Finally, the dynamic effects of miR-138 and p65 were detected to investigate whether miR-138 exerts its biological functions through targeting RELA. In summary, we attempt to search for miRNA that could target RELA, therefore improving the trophoblast dysfunction during preeclampsia.

Materials and methods

Clinical sampling

A total of 12 preeclampsia placenta tissues were obtained from pregnant women complicated by preeclampsia and a total of 12 normal placenta tissues were obtained from physiological pregnant women. All women were enrolled voluntarily with signed informed consent. The sampling was performed with the approval of the Ethics Committee of the Nanfang Hospital, Southern Medical University (Approval No.NFEC-2017-103). De novo hypertension (blood pressure >140/90 mm Hg) and proteinuria (>300 mg/day) after 20 weeks of gestation were used to diagnose preeclampsia. Women with NP had singleton pregnancies and no evidence of preeclampsia or previous hypertensive disorders. Pregnancy evolution was monitored from 22 to 38 weeks of pregnancy accordingly [26,27].

Cell lines

An immortalized human trophoblast cell line, HTR-8/SVneo (ATCC[®] CRL-3271[™]), was obtained from ATCC (Manassas, VA, USA) and cultured in RPMI-1640 Medium (Invitrogen, Carlsbad, CA, USA) supplemented with 5% FBS. A human chorionicarcinoma cell line, JEG-3 (ATCC[®] HTB-36[™]), was obtained from ATCC and cultured in Eagle's Minimum Essential Medium (Invitrogen) supplemented with 10% FBS. All cells were cultured at 37°C in 5% CO₂.

Bioinformation analysis

GEO datasets GSE96983 (Different expression profiles of miRNAs in preeclampsia and normal placenta) and GSE103542 (Dysregulated Placental microRNA in early and late-onset preeclampsia) was downloaded. R package Limma was used for analyzing the different expression miRNAs ($|\log_{2}FC| > 0.56$, $P < 0.05$). Online prediction tools DIANA TOOLS (<http://www.microrna.gr/microT-CDS/>), TargetScan (http://www.targetscan.org/vert_72/), mirDIP (<http://ophid.utoronto.ca/mirDIP/index.jsp>) and StarBase (<http://starbase.sysu.edu.cn/index.php>) were used for analyzing the target genes of miR-138-5p.

Cell transfection

The overexpression or inhibition of miR-138 was achieved by transfecting agomir-138 or antagomir-138; agomir-NC or antagomir-NC was used as a negative control. The silencing of p65 was achieved by transfecting sh-p65 vector; sh-NC vector was used as a negative control. The overexpression of p65 was achieved by transfecting pcDNA3.1/p65; empty pcDNA3.1 was used as a negative control. All the transfection vectors or miRNAs were obtained from GenePharm (Shanghai, China). 1 $\mu\text{g}/\text{ml}$ vector or 50 nm gomir/antagomir were transfected into HTR-8/SVneo or JEG-3 cells using Lipofectamine 3000 (Invitrogen). After 6 h, the medium was replaced with fresh complete medium. Cells were harvested for further investigation after 48 h of transfection. The primers for plasmid construction are listed in Table S1.

Hematoxylin and eosin (H&E) staining

Collected placental tissues were paraffin-embedded, sliced into 4- μm thick sections, and routinely dewaxed with dimethylbenzene. Then, the slices were washed and stained by hematoxylin for 15 min, treated with 1% hydrochloric acid alcohol, and stained with eosin staining solution. Then, gradient alcohol (80% ethanol for 2 sec, 95% ethanol for 3 min and absolute alcohol for 6 min) was used for slices dehydration. Xylene was used for slices trans-

parent. The sections were observed under a microscope.

Polymerase chain reaction (PCR)-based examination

The extraction of total RNA from target tissues and cells was performed using a TRIzol reagent (Thermo Fisher Scientific, Waltham, MA, USA). The cDNA synthesis was performed using an ABScript II cDNA First-Strand synthesis kit (ABclonal Biotech, Wuhan, China). The expression levels of mRNA and miRNA were examined using an SYBR Green PCR Master Mix (Qiagen, Hilden, Germany). For calculating the relative expression levels of mRNA or miRNA, the $2^{-\Delta\Delta C_t}$ method was used [28] taking GAPDH or U6 expression as an internal reference. The primers are listed in Table S1.

Transwell assay

For invasion examination, cells were planted on the top side of polycarbonate Transwell filters coated with Matrigel at a density of 5×10^5 cells/well. The medium without serum was used in the top chambers and medium with serum was used in the bottom chamber. After incubating the cells at 37°C for 48 h, use a cotton swab to remove noninvasive cells from the apical compartment. Invasive cells on the surface of the bottom compartment membrane were fixed in 100% methanol for 10 minutes, air-dried, stained with crystal violet solution, and then observed and counted under a microscope.

Wound healing assay

Cells (5×10^5 cells/ml) were seeded in 6-well plates. When the cell monolayer emerged, cells were treated with mitomycin C (1 $\mu\text{g}/\text{ml}$) for 1 h. Then, a scratch was made using a sterile toothpick perpendicularly to the plane of the cell. After the scratch is completed, wash the non-adherent cells to make the gap clearly visible. At 0 or 48 h of the scratching, the width of the scratch was measured under a microscope (Olympus, Japan) and the relative distance of cell

migration to the scratch area was calculated using the ImageJ software (NIH, USA).

Immunohistochemical (IHC) staining

Collected placental tissues were paraffin-embedded, sliced into 4- μ m thick sections, and routinely dewaxed and rehydrated, washed in PBS, and incubated in H₂O₂ in methanol for 30 min at room temperature to block endogenous peroxidase. The nonspecific proteins were blocked by an incubation with 5% normal goat serum for 30 min at room temperature. Then, the serum was discarded and the slices were incubated with polyclonal primary antibody against p65 (10,745-1-AP; Proteintech, Wuhan, China) or the blocking serum (as negative control) overnight at 4°C. At the end of the incubation, the slides were then washed and stained with rabbit IgG-immunohistochemical SABC kit (Boster, Wuhan, China). After washing with PBS, hematoxylin was added for nuclei staining (0.1% Mayer's hematoxylin). Then a standard dehydration, transparent and mount procedure, the slides were observed by microscope.

Immunoblotting

After harvesting the cells, a proper amount of ice-precooled lysis buffer was added and cells were put onto the ice for 10–20 minutes to lyse the cells. The cells were collected and centrifuged at 12,000 g for 4 min at 4°C. The protein sample concentration was measured by a BCA protein assay kit (Beyotime, Shanghai, China) method and then adjusted to a uniform concentration. Protein samples were separated by 10% sodium dodecyl sulfate-polyacrylamide gel electrophoresis and then transferred onto a polyvinylidene fluoride membrane (Millipore, Billerica, MA, USA). Before incubating with the primary antibodies, the nonspecific binding was blocked by incubating the cells with 5% skimmed milk at room temperature for 2 h. After that, the membrane was incubated with anti-p65 (10,745-1-AP; Proteintech) or anti-GAPDH (T0004; Affinity, Cincinnati, OH, USA) at 4°C overnight followed by another incubation with the proper secondary antibody at room temperature for 1 h. GAPDH was taken as an internal

reference. The visualization of the blots was performed using a BeyoECL Plus kit (Beyotime) and the signal was analyzed by the Amersham ECL Western Blotting System (GE Healthcare, Chicago, IL, USA).

Dual-luciferase reporter assay

For validating the binding between p65 (RELA) and miR-138-5p, we performed the dual-luciferase reporter assay. Wild- and mutant-type RELA 3'-UTR luciferase reporter plasmids were constructed (wt-RELA and mut-RELA) by cloning the wild or mutated RELA 3'-UTR to the downstream of the Renilla psi-CHECK2 plasmid (Promega, Madison, WI, USA). These reporter plasmids were co-transfected in 293 T cells with agomir-138/antagomir-138 and the luciferase activity was determined using the Dual-Luciferase Reporter Assay System (Promega). The primers for plasmid construction are listed in Table S1.

AGO2 assay

The Magna RIP RNA-Binding Protein Immunoprecipitation Kit (Millipore) was used to assess the interaction of the miR-138-5p, RELA 3'UTR with AGO2 following the manufacturer's specifications. Briefly, use a lysis buffer containing a protease inhibitor cocktail and RNase inhibitor to lyse the HTR-8/SVneo cells. Pre-incubate the magnetic beads with human anti-Ago2 (ab32381, Abcam) or anti-IgG (negative control) for 30 min at room temperature. Incubate the cell lysates with the Ago2- or IgG-beads complex overnight at 4°C. At the end of the incubation, the RNA was precipitated, purified, reverse transcribed, and the levels of miR-135-5p and 3'UTR of RELA were detected by qRT-PCR. We used Δ Ct values for determining enrichment fold change relative to IgG controls. The primers for plasmid construction are listed in Table S1.

Data processing and statistical analysis

Use GraphPad software to analyze the data. Data from all the assays were expressed as mean \pm standard deviation (SD). All the data were analyzed by normality test using Kolmogorov-Smirnov test. Student's *t*-test was used to compare the normality data between two groups. The one-way

ANOVA follows post hoc Turkey's test was used to compare the normality data among more than two groups. Whitney U test for the non-parametric data. A *P* value of less than 0.05 was considered statistically significant.

Results

miR-138-5p expression within tissue samples and cells

First, we analyzed the GEO dataset GSE96983 and GSE103542 using R package Limma ($|\log_{2}FC| > 0.56$, $P < 0.05$). In GSE96983, 28 miRNAs were downregulated, 15 miRNAs were upregulated in preeclampsia placenta tissues, compared to normal placenta tissues (Figure S1A). In GSE103542, 41 miRNAs were downregulated, 37 miRNAs were upregulated in late preeclampsia placenta tissues, compared to early preeclampsia placenta tissues (Figure S1B). We intersected the downregulated miRNAs from the two GEO dataset (Table S2 and S3) and found miR-138-5p (Figure 1(a)). Later, we validated the expression level of miR-138-5p within tissues and trophoblasts upon LPS stimulation. According to GSE96983 and GSE103542, miR-138-5p expression showed to be dramatically decreased within preeclampsia placenta (PE) tissues or late stage PE tissues compared with normal placenta tissues or the early stage PE tissues (Figure 1(b)). Then, normal and PE placenta tissues were collected and the histopathological characteristics were examined using H&E staining. As shown in Figure 1(c), several spiral arteries with large lumen and thin walls were found in placental tissues of preeclampsia (Figure 1(c)). In PE placenta tissues ($n = 12$), miR-138-5p expression showed to be dramatically downregulated than that within normal placenta tissue samples ($n = 12$) (Figure 1(d)). Moreover, an immortalized human trophoblast cell line, HTR-8/SVneo, and a human choriocarcinoma cell line, JEG-3, showed to be exposed to 100 ng/ml LPS for 24 h and examined for miR-138-5p expression; Figure 1(e) shows that, in both these cells, the expression level of miR-138-5p was dramatically decreased by LPS stimulation.

Specific effects of miR-138-5p upon trophoblast invasion and migration

After confirming that miR-138-5p was abnormally downregulated within PE placenta and LPS-stimulated trophoblasts, next, we achieved miR-138 overexpression or inhibition within both HTR-8/SVneo and JEG-3 cell lines by transfecting agomir-138 or antagomir-138 for functional experiments. The transfection efficiency was verified by real-time qPCR (Figure 2(a)). Then, agomir-138-transfected cells were exposed to LPS and examined for inflammatory factor levels, cell migration, and cell invasion. In both cell lines, miR-138 overexpression downregulated TNF- α and IL-6 mRNA expression (Figure 2(b)), whereas promoted migratory ability (Figure 2(c)) and invasive ability (Figure 2(d)) of cells; LPS stimulation exerted opposite effects (Figure 2(b-d)). More importantly, miR-138 overexpression partially reversed the effects of LPS stimulation, suggesting that miR-138 overexpression could improve inflammation and oxidative stress caused by LPS.

miR-138-5p directly binds to 3'UTR of RELA

Online prediction tools DIANA TOOLS, TargetScan, mirDIP and StarBase were used to predict the miR-138-5p targeted genes. There are 15 candidate genes (Figure S1C). Among them, RELA have been reported to be highly expressed in preeclampsia placentas and trigger endothelial dysfunction in preeclamptic women [13,14,29]. Herein, IHC staining showed that p65-positive cases were higher in PE pregnancies than those within control pregnancies (Figure 3(a)); further Immunoblotting also revealed that p65 protein contents showed to be significantly upregulated within PE placenta tissue samples than those within normal placenta tissue samples (Figure 3(b)). Consistently, in LPS-stimulated HTR-8/SVneo and JEG-3 cell lines, p65 protein contents showed to be dramatically increased than those in non-stimulated HTR-8/SVneo and JEG-3 cell lines (Figure 3(c)). Thus, LPS could indeed induce p65 expression in trophoblasts.

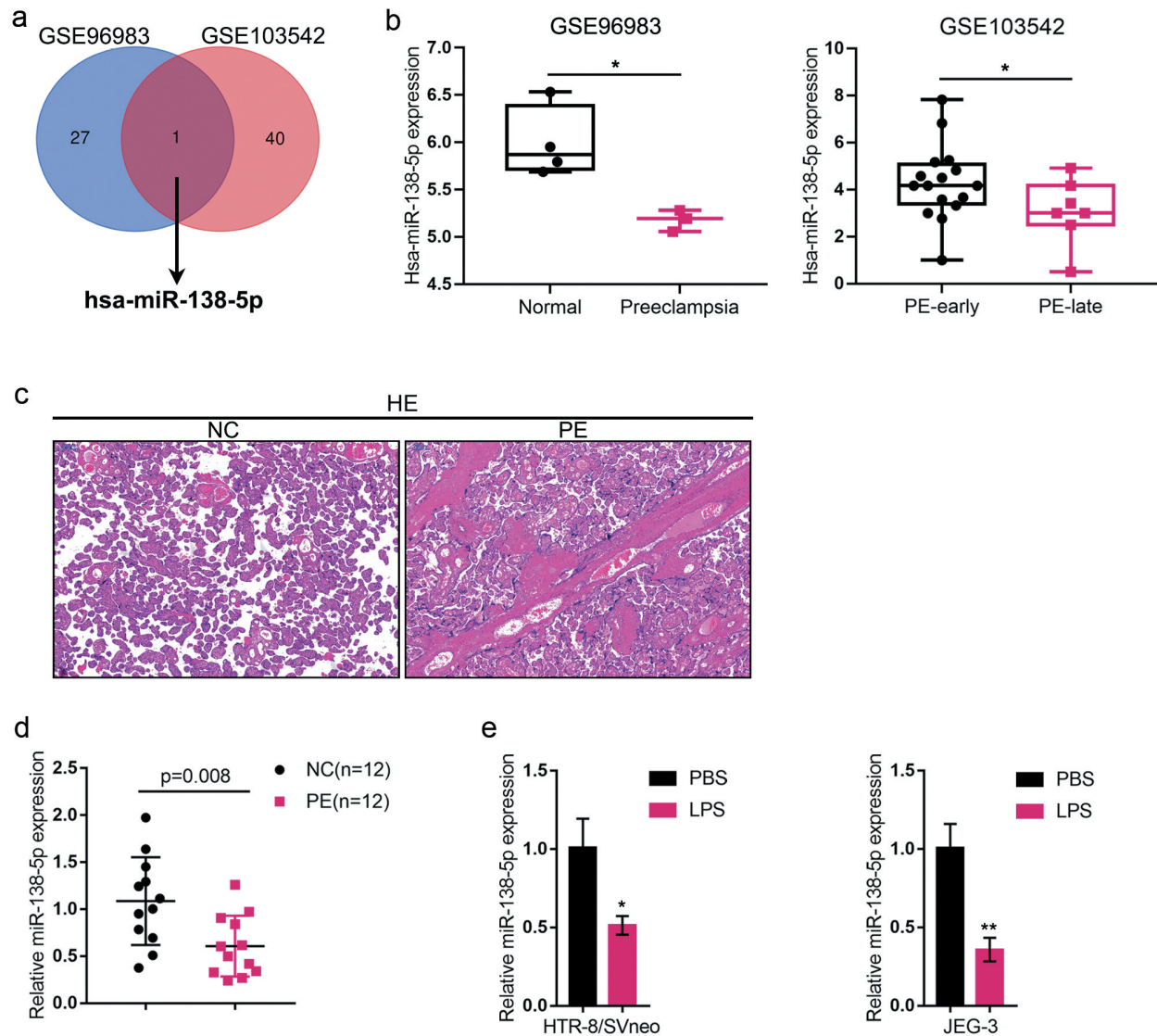


Figure 1. Expression of miR-138-5p in tissue samples and cells (a) The different expressed miRNAs in GSE96983 (Different expression profiles of miRNAs in preeclampsia and normal placenta) and GSE103542 (dysregulated placental microRNAs in early and late onset preeclampsia) were analyzed by R package Limma ($|\log_{2}FC| > 0.56$, $P < 0.05$). There are 28 and 41 downregulated miRNAs in preeclampsia or in late preeclampsia placenta tissues. MiR-138-5p was selected by the intersection of those two GEO dataset. (b) miR-138-5p expression in normal and preeclampsia placenta tissue (GSE96983) and in the early stage and late stage preeclampsia placenta (PE) tissues (GSE103542). (c) The histopathological characteristics of normal and PE placenta tissues were examined using hematoxylin and eosin (H&E) staining. (d) miR-138-5p expression was examined in normal ($n = 12$) and PE placenta tissues ($n = 12$) by real-time qPCR. (e) An immortalized human trophoblast cell line, HTR-8/SVneo, and a human choriocarcinoma cell line, JEG-3, were exposed to 100 ng/ml LPS for 24 h and examined for the expression of miR-138-5p by real-time qPCR. * $P < 0.05$, ** $P < 0.01$.

Since miR-138-5p has been predicted to target p65, next, HTR-8/SVneo and JEG-3 cell lines were transfected with agomir-138/antagomir-138 and examined for the protein levels of p65; Figure 3(d–e) showed that the overexpression of miR-138 decreased, while the inhibition of miR-138 increased p65 protein levels. Then, we constructed two different types of RELA 3'-UTR luciferase reporter plasmids, wild-type and mutant-type. We co-transfected these

luciferase reporter plasmids in 293 T cells with agomir-138/antagomir-138, and examined for the luciferase activity. Figure 3(f) shows that the overexpression of miR-138 dramatically downregulated, while the inhibition of miR-138 upregulated wt-RELA luciferase activity; when co-transfected with mut-RELA, agomir-138 or antagomir-138 transfection failed to alter the luciferase activity of mut-RELA. Moreover, the AGO2 assays confirmed that miR-

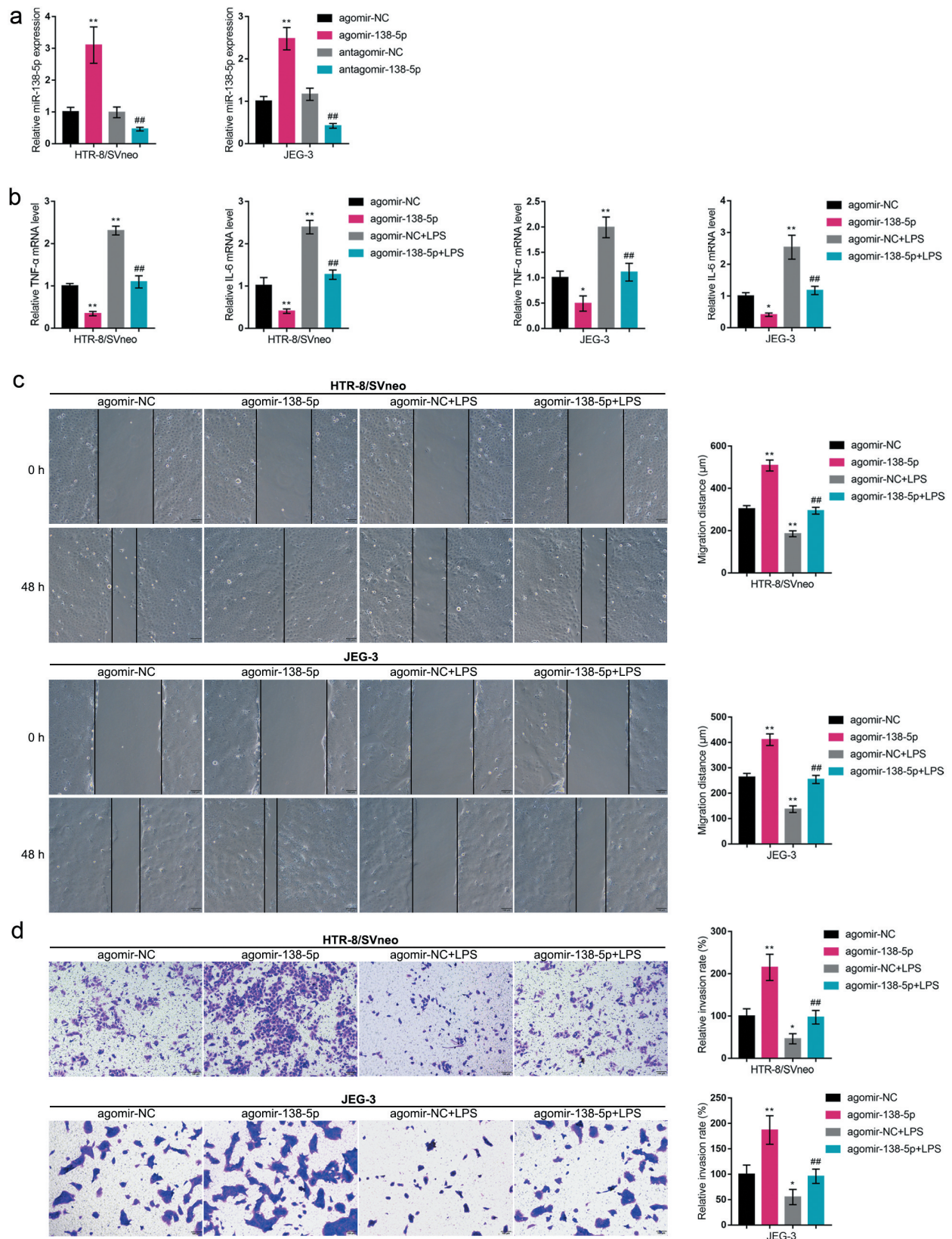


Figure 2. Specific effects of miR-138-5p on trophoblast invasion and migration (a) HTR-8/SVneo and JEG-3 cells were transfected with agomir-138 or antagomir-138 for miR-138 overexpression or inhibition; the transfection efficiency was verified by real-time qPCR. Then, HTR-8/SVneo and JEG-3 cells were transfected with agomir-138, exposed to LPS, and examined for the mRNA expression levels of TNF- α and IL-6 by real-time qPCR (b); cell migration by Wound healing assay (c); cell invasion by Transwell assay (d). * $P < 0.05$, ** $P < 0.01$, compared with the control group; ## $P < 0.01$, compared with the agomir-NC + LPS group.

138-5p and RELA 3'UTR levels were higher in anti-Ago2 immunoprecipitate compared to anti-IgG immunoprecipitate (Figure 3(g)). These data indicate that miR-138 directly binds RELA 3'-UTR to inhibit p65 expression.

In vitro effects of p65 on trophoblast migration and invasion

Since p65 is abnormally upregulated in LPS-stimulated trophoblasts, next, we conducted p65 silencing within HTR-8/SVneo and JEG-3 cell lines

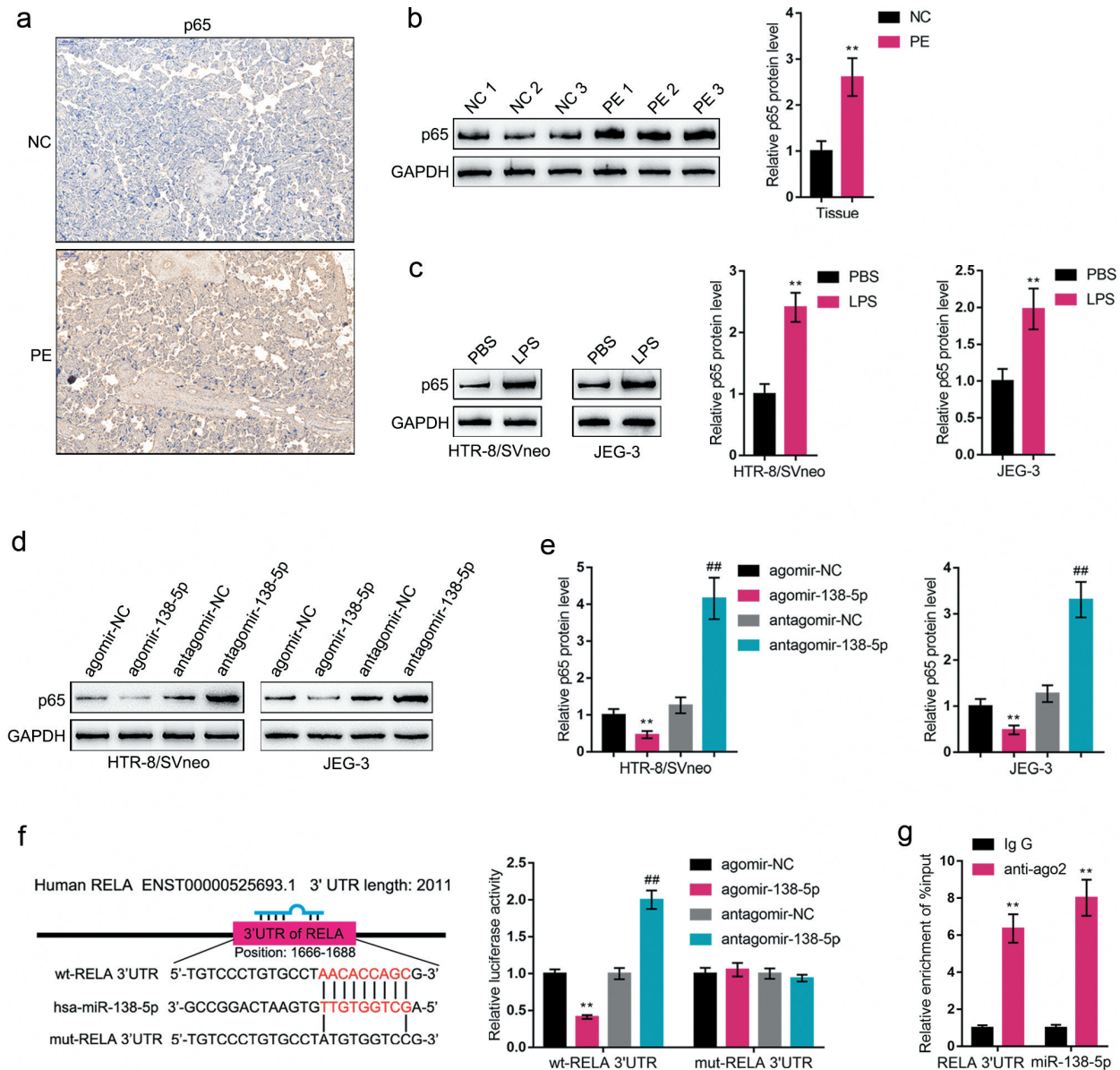


Figure 3. P65 is a direct downstream target of miR-138-5p (a) The protein content and distribution of p65 were determined in normal and PE placenta tissues by Immunohistochemical (IHC) staining. (b) The protein levels of p65 were determined in normal and PE placenta tissues by Immunoblotting. (c) HTR-8/SVneo and JEG-3 cells were stimulated with LPS and examined for the protein levels of p65 by Immunoblotting. (d-e) HTR-8/SVneo and JEG-3 cells were transfected with agomir-138 or antagomir-138 and examined for the protein levels of p65 by Immunoblotting. (f) Wild-type and mutant-type RELA 3'-UTR luciferase reporter plasmids were constructed and co-transfected in 293 T cells with agomir-138/antagomir-138; the luciferase activity was determined. (g) AGO2 assay was performed using anti-IgG or anti-Ago2. The levels of miR-138-5p and RELA 3'UTR in immunoprecipitate were determined by qRT-PCR. ** $P < 0.01$, ## $P < 0.01$.

by transfecting small hairpin RNA for p65 (sh-p65), as confirmed by real-time qPCR and Immunoblotting (Figure 4(a-b)). Then, we transfected HTR-8/SVneo and JEG-3 cell lines by sh-p65, exposed these cells to LPS, and examined for related indexes. As for the inflammatory factors, LPS-induced increases in TNF- α and IL-6 mRNA expression showed to be significantly reduced via p65 silencing (Figure 4(c)). As for the cellular functions, LPS stimulation inhibited cell migration (Figure 5(a)) and cell invasion (Figure 5(b)), whereas p65 silencing exerted opposite effects (Figure 5(a-b)); p65 silencing significantly attenuated the functions of LPS stimulation (Figure 5(a-b)). In summary, p65 silencing might also improve LPS-stimulated inflammation and oxidative stress.

miR-138 modulates cell migration, invasion, and inflammatory factors through p65

Since miR-138 directly binds to p65, finally, we co-transfected HTR-8/SVneo and JEG-3 cell lines with

pcDNA3.1/p65 and agomir-138 to detect the dynamic effects of the miR-138/p65 axis on LPS-induced inflammation and oxidative stress. Within both cells, p65 protein contents showed to be down-regulated via the overexpression of miR-138 and upregulated via the overexpression of p65; the functions of miR-138 overexpression were partially reversed by p65 overexpression (Figure 6(a)). Next, co-transfected HTR-8/SVneo and JEG-3 cell lines were exposed to LPS and examined for related indexes. As for the inflammatory factors, miR-138 overexpression inhibited, whereas p65 overexpression promoted TNF- α and IL-6 mRNA expression (Figure 6(c)); the effects of miR-138 overexpression were partially reversed by p65 overexpression (Figure 6(c)). Under LPS stimulation, miR-138 overexpression promoted the cell migratory ability (Figure 7(a)) and invasive ability (Figure 7(b)), whereas p65 overexpression exerted opposite effects (Figure 7(a-b)); p65 overexpression significantly attenuated the functions of miR-138 overexpression (Figure 7(a-b)). These data indicate that miR-138

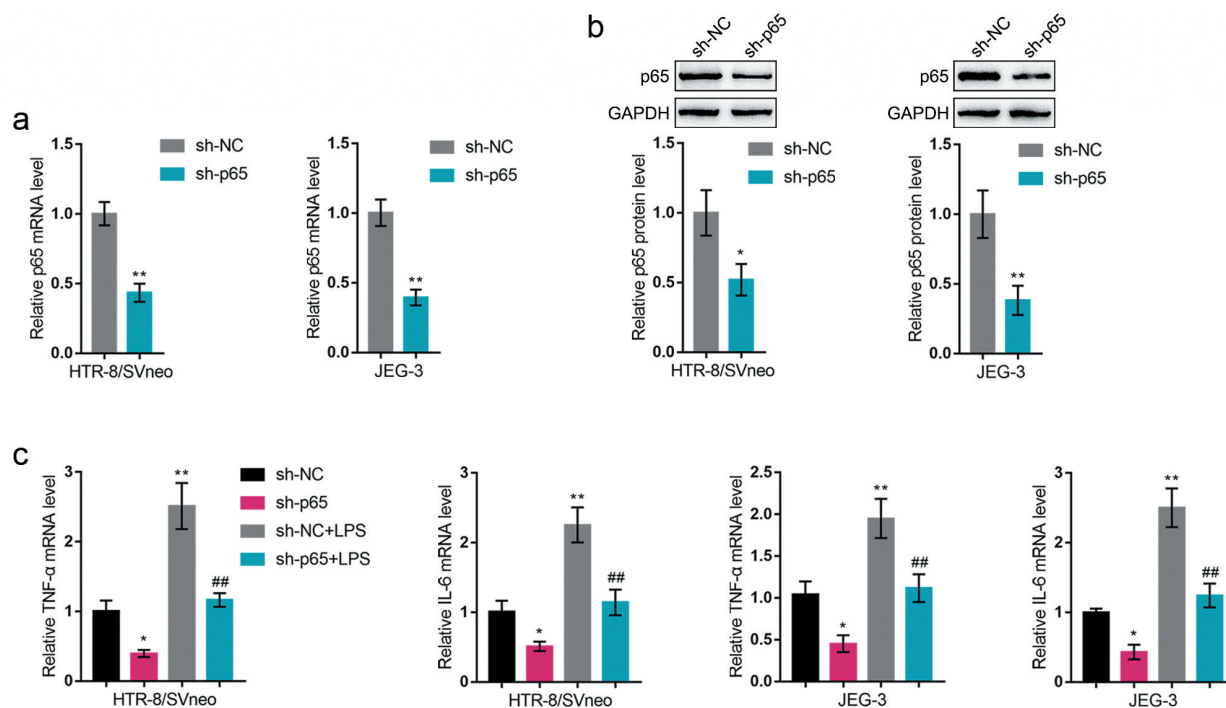


Figure 4. *In vitro* effects of p65 on trophoblast inflammatory factors (a-b) P65 silencing was achieved in HTR-8/SVneo and JEG-3 cells by transfecting small hairpin RNA for p65 (sh-p65); the transfection efficiency was verified by real-time qPCR and Immunoblotting. Then, HTR-8/SVneo and JEG-3 cells were transfected by sh-p65, exposed to LPS, and examined for the mRNA levels of TNF- α and IL-6 by real-time qPCR (c). * $P < 0.05$, ** $P < 0.01$, compared with the control group; ## $P < 0.01$, compared with the sh-NC + LPS group.

overexpression attenuates LPS-induced inflammation and oxidative stress through targeting p65.

Discussion

Herein, the study identified the miR-138/RELA axis modulating the migratory and invasive ability

of HTR-8/SVneo and JEG-3 cells, as well as the inflammatory factor levels in response to LPS stimulation. miR-138 expression was upregulated in preeclampsia placenta and LPS-stimulated HTR-8/SVneo and JEG-3 cell lines. miR-138 overexpression rescued the migratory ability and invasive ability of HTR-8/SVneo and JEG-3 cells inhibited

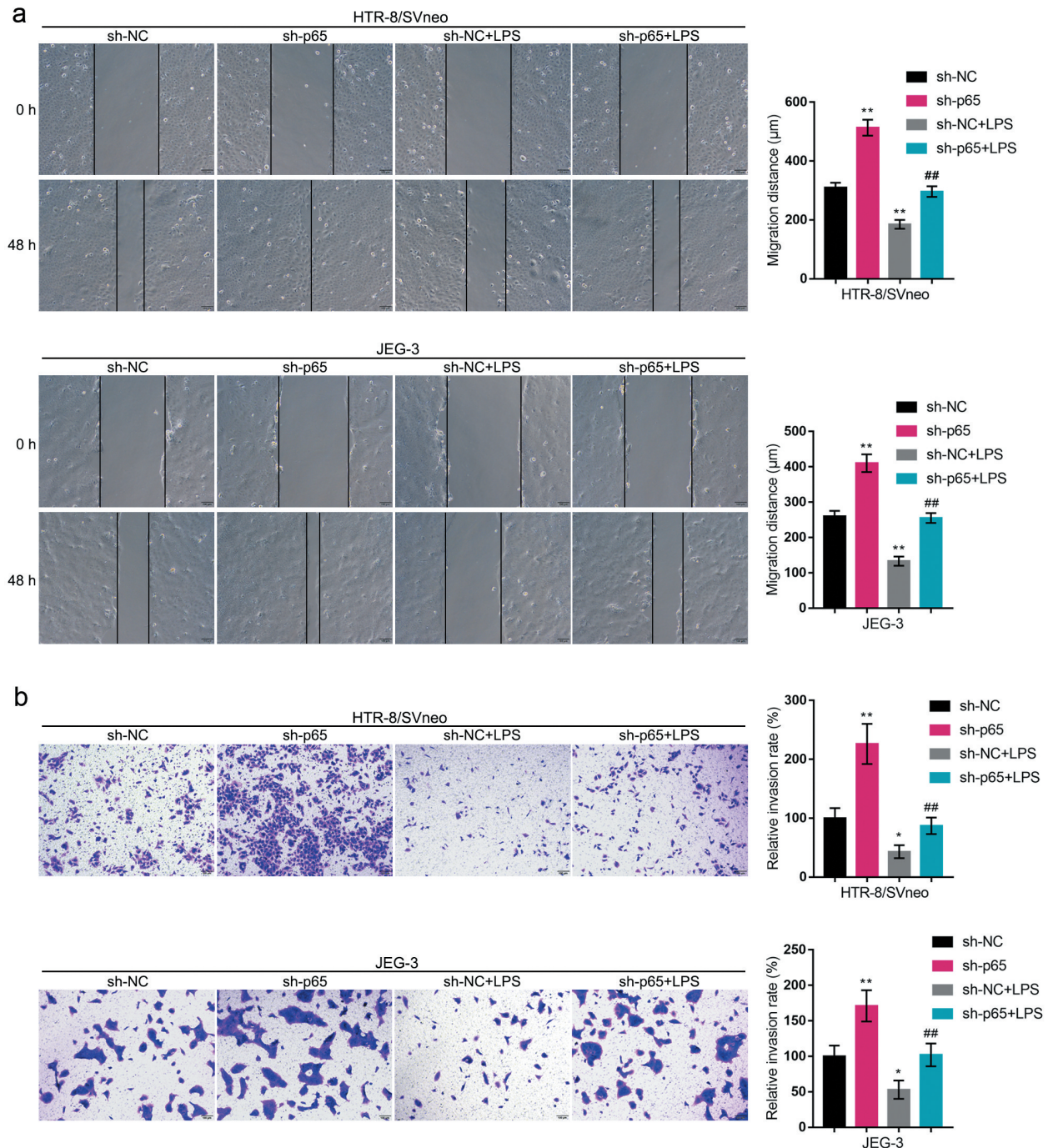


Figure 5. *In vitro* effects of p65 on trophoblast migration and invasion HTR-8/SVneo and JEG-3 cells were transfected by sh-p65, exposed to LPS, and examined for cell migration by Wound healing assay (a) and cell invasion by Transwell assay (b). * $P < 0.05$, ** $P < 0.01$, compared with the control group; ## $P < 0.01$, compared with the sh-NC + LPS group.

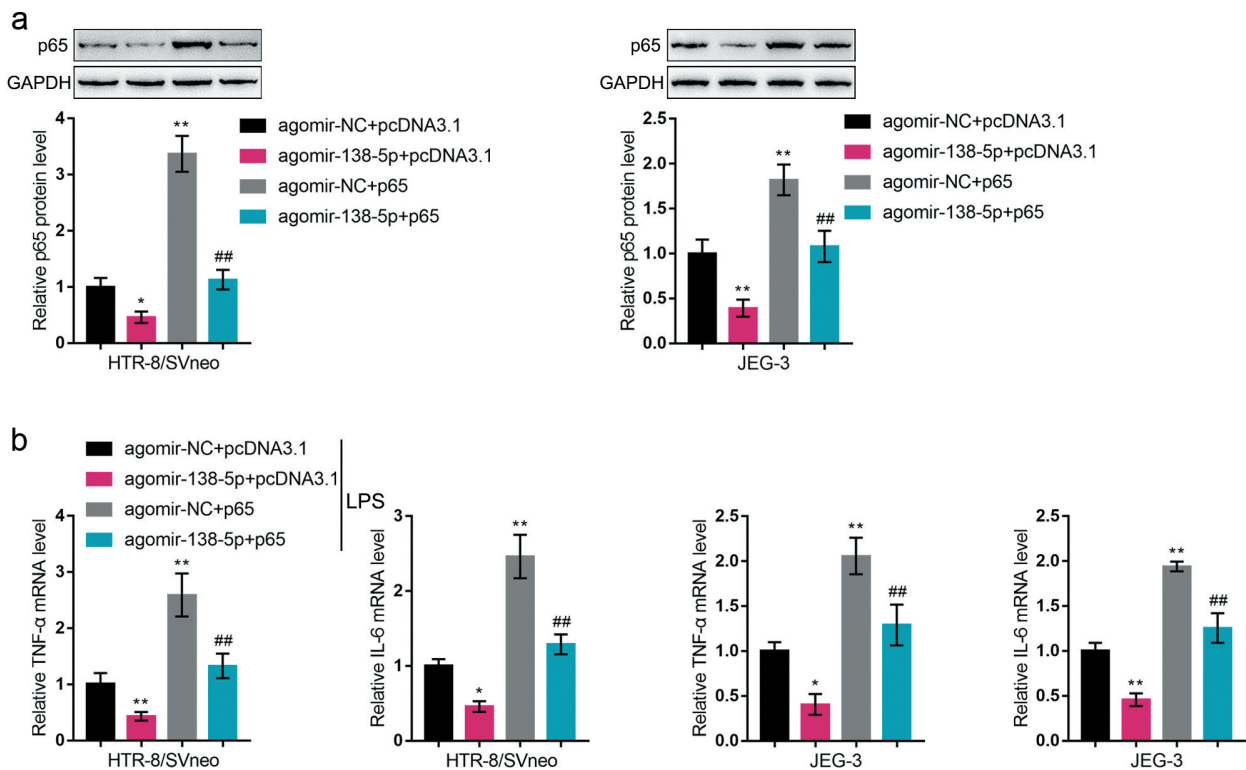


Figure 6. Dynamic effects of miR-138 and p65 on p65 and inflammatory factors (a) HTR-8/SVneo and JEG-3 cells were co-transfected by pcDNA3.1/p65 and agomir-138 and examined for the protein levels of p65 by Immunoblotting. Then, HTR-8/SVneo and JEG-3 cells were co-transfected by pcDNA3.1/p65 and agomir-138, exposed to LPS, and examined for the mRNA levels of TNF- α and IL-6 by real-time qPCR (b). * $P < 0.05$, ** $P < 0.01$, compared with the control group; ## $P < 0.01$, compared with the agomir-NC + p65 group.

by LPS stimulation, and decreased LPS-induced TNF- α and IL-6 levels. By binding the 3'-UTR of RELA, miR-138 negatively regulated p65 expression. The silencing of p65 also improved LPS-induced HTR-8/SVneo and JEG-3 cell dysfunction and TNF- α and IL-6 levels. More importantly, p65 overexpression partially reversed the functions of miR-138 overexpression upon both cells, indicating that miR-138 exerted its biological effects through targeting RELA.

Aberrant placental miRNA expression was found to be implicated in preeclampsia. Timofeeva et al. [20] reported that the expression levels of miR-532-5p, -423-5p, -127-3p, -539-5p, -519a-3p, and -629-5p and let-7 c-5p were decreased by more than two-fold within the placenta, whereas the expression levels of miR-423-5p, 519a-3p, and -629-5p and let-7 c-5p were increased by more than two-fold within the blood plasma of pregnancy with preeclampsia; moreover, miR-423-5p was proposed as an underlying candidate for the early diagnosis of preeclampsia in

the process of targeted therapies for high-risk pregnancy. Herein, miR-138 expression was found significantly downregulated in preeclampsia placenta, as well as within HTR-8/SVneo and JEG-3 cell lines upon LPS stimulation, suggesting that miR-138 could be involved in preeclampsia pathogenesis through modulating trophoblast functions and inflammation in placenta.

miRNAs could participate in multiple events during trophoblast dysfunction and preeclampsia. miR-30a-3p, which showed to be overexpressed within the preeclampsia placentas, could alter JEG-3 cell invasion and elicit HTR-8/SVneo cell apoptosis [30]. Another elevated miRNA in the preeclamptic placental specimens, miR-320a, also remarkably suppressed trophoblast invasion [31] and growth [32]. In contrast to miR-30a-3p and miR-320a, miR-218-5p exhibited a high expression level within extra villous trophoblasts and a dramatically decreased expression level within the placentas of preeclampsia. The overexpression of miR-218-

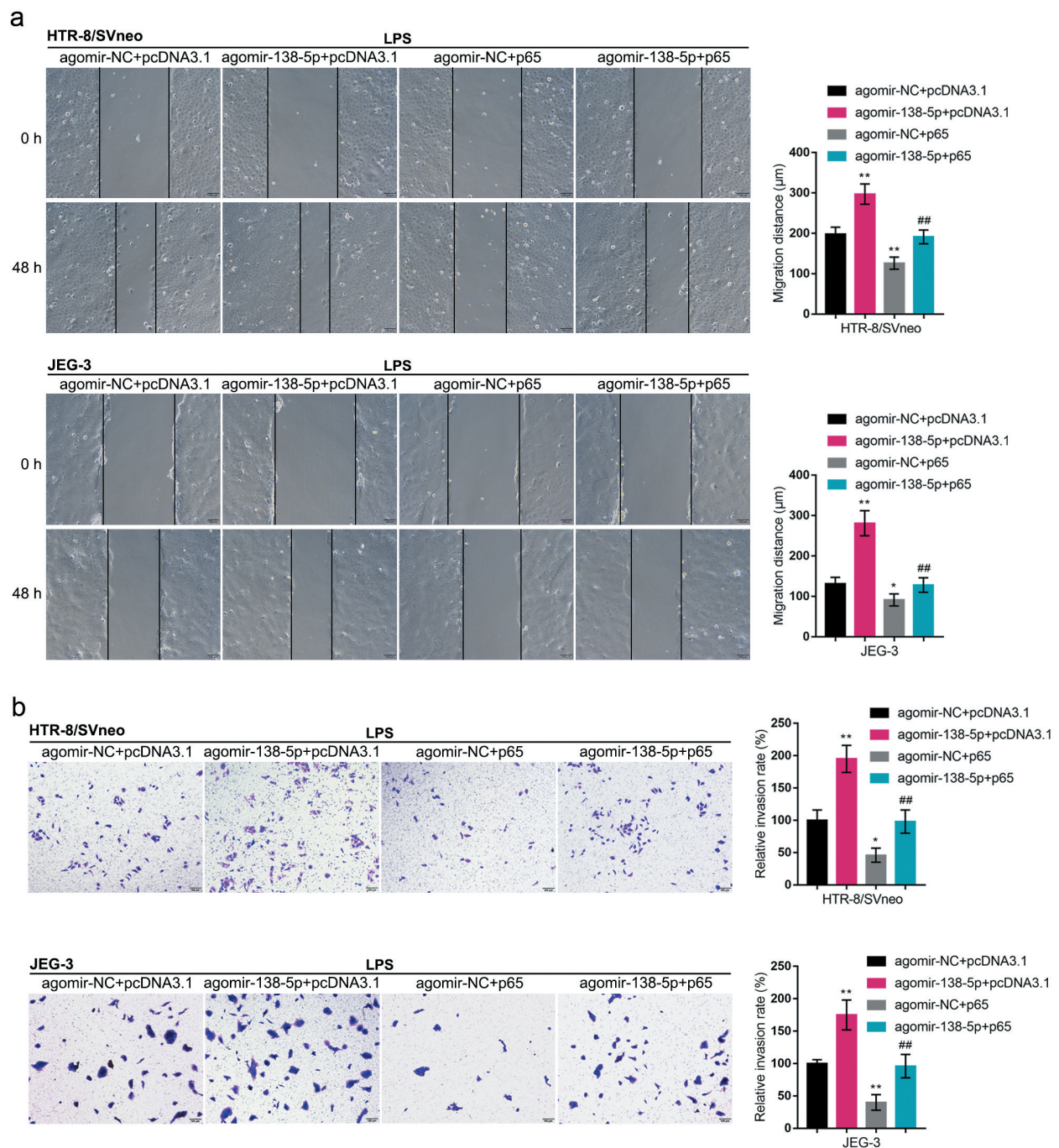


Figure 7. Dynamic effects of miR-138 and p65 on trophoblast migration and invasion. HTR-8/SVneo and JEG-3 cells were co-transfected by pcDNA3.1/p65 and agomir-138, exposed to LPS, and examined for the cell migration by Wound healing assay (a) and the cell invasion by Transwell assay (b). * $P < 0.05$, ** $P < 0.01$, compared with the control group; ## $P < 0.01$, compared with the agomir-NC + p65 group.

5p increased, while anti-miR-218-5p reduced the invasive ability of trophoblasts, and the outgrowth and differentiation of extra villous trophoblasts [33]. Herein, miR-138 overexpression in LPS-stimulated trophoblasts also enhanced cell migratory and invasive ability, indicating that rescuing

miR-138 expression might attenuate trophoblast dysfunction during preeclampsia.

In addition to trophoblast behaviors, miR-138 overexpression significantly reduced LPS-induced inflammatory factor levels, including TNF- α and IL-6. Considering that miR-138 has been predicted as an

upstream regulator of RELA, miR-138 might exert its effects through inflammation signaling pathways. As we have mentioned, by binding to complementary “seed” regions of mRNAs, mature miRNAs could induce mRNA degradation and translational repression, thus preventing protein formation [17]. miRNAs reviewed above, including miR-30a-3p, miR-320a, and miR-31-5p, all exert their effects in preeclampsia through targeting different downstream mRNAs. miR-30a-3p acts on trophoblasts through targeting IGF-1 [30], miR-320a through estrogen-related receptor-gamma [31] and IL4 [32], and miR-31-5p through eNOS [25]. Herein, both the bioinformatics and experimental analyses indicated that miR-138 directly bound RELA 3'-UTR, leading to the downregulation of p65 expression and protein levels.

The effects of NF- κ B on placenta inflammation and preeclampsia development have been widely reported. Numerous studies indicated the activation of NF- κ B signaling in preeclampsia [13,34–34–38]. Herein, we also observed increased p65 protein in preeclampsia placenta and trophoblasts in response to LPS stimulation. Similar as miR-138 overexpression, p65 silencing rescued HTR-8/SVneo and JEG-3 cell migration and invasion, as well as decreased TNF- α and IL-6 levels. More importantly, p65 overexpression exerted opposite effects on trophoblasts and inflammatory factors, and dramatically attenuated the effects of miR-138 overexpression upon trophoblasts and inflammatory factors, indicating that miR-138 exerts its functions through targeting RELA.

In conclusion, miR-138 improves LPS-induced inflammation and oxidative stress on trophoblasts through targeting RELA and affecting NF- κ B signaling. The miR-138/RELA axis might be involved in preeclampsia pathogenesis, which requires further *in vivo* and clinical researches.

Disclosure statement

No potential conflict of interest was reported by the authors.

Funding

This study was supported by National Natural Science Foundation of China (81671466) and President Foundation of Nanfang Hospital, Southern Medical University (no. 2020B015).

References

- [1] Catarino C, Santos-Silva A, Belo L, et al. Inflammatory disturbances in preeclampsia: relationship between maternal and umbilical cord blood. *J Pregnancy*. 2012;2012:684384.
- [2] Matsubara K, Matsubara Y, Hyodo S, et al. Role of nitric oxide and reactive oxygen species in the pathogenesis of preeclampsia. *J Obstet Gynaecol Res*. 2010;36(2):239–247.
- [3] Matsubara K, Higaki T, Matsubara Y, et al. Nitric oxide and reactive oxygen species in the pathogenesis of preeclampsia. *Int J Mol Sci*. 2015;16(3):4600–4614.
- [4] Brosens I, Renaer M. On the pathogenesis of placental infarcts in pre-eclampsia. *J Obstet Gynaecol Br Commonw*. 1972;79(9):794–799.
- [5] Meekins JW, Pijnenborg R, Hanssens M, et al. A study of placental bed spiral arteries and trophoblast invasion in normal and severe pre-eclamptic pregnancies. *Br J Obstet Gynaecol*. 1994;101(8):669–674.
- [6] Myatt L. Role of placenta in preeclampsia. *Endocrine*. 2002;19(1):103–111.
- [7] Redline RW, Patterson P. Pre-eclampsia is associated with an excess of proliferative immature intermediate trophoblast. *Hum Pathol*. 1995;26(6):594–600.
- [8] de Groot CJ, O'Brien TJ, Taylor RN. Biochemical evidence of impaired trophoblastic invasion of decidual stroma in women destined to have preeclampsia. *Am J Obstet Gynecol*. 1996;175(1):24–29.
- [9] Conrad KP, Miles TM, Benyo DF. Circulating levels of immunoreactive cytokines in women with preeclampsia. *Am J Reprod Immunol*. 1998;40(2):102–111.
- [10] Gilbert JS, Ryan MJ, LaMarca BB, et al. Pathophysiology of hypertension during preeclampsia: linking placental ischemia with endothelial dysfunction. *Am J Physiol Heart Circ Physiol*. 2008;294(2):H541–50.
- [11] Lee KS, Kim J, Kwak S-N, et al. Functional role of NF-kappaB in expression of human endothelial nitric oxide synthase. *Biochem Biophys Res Commun*. 2014;448(1):101–107.
- [12] Xie C, Yao MZ, Liu JB, et al. A meta-analysis of tumor necrosis factor-alpha, interleukin-6, and interleukin-10 in preeclampsia. *Cytokine*. 2011;56(3):550–559.
- [13] Vaughan JE, Walsh SW. Activation of NF-kappaB in placentas of women with preeclampsia. *Hypertens Pregnancy*. 2012;31(2):243–251.
- [14] Kim J, Lee K-S, Kim J-H, et al. Aspirin prevents TNF-alpha-induced endothelial cell dysfunction by regulating the NF-kappaB-dependent miR-155/eNOS pathway: role of a miR-155/eNOS axis in preeclampsia. *Free Radic Biol Med*. 2017;104:185–198.
- [15] Li G, Ma L, Lin L, et al. The intervention effect of aspirin on a lipopolysaccharide-induced preeclampsia-like mouse model by inhibiting the nuclear factor-kappaB pathway. *Biol Reprod*. 2018;99(2):422–432.

- [16] Jeyaseelan K, Herath WB, Armugam A. MicroRNAs as therapeutic targets in human diseases. *Expert Opin Ther Targets*. 2007;11(8):1119–1129.
- [17] Barik S. Silence of the transcripts: RNA interference in medicine. *J Mol Med (Berl)*. 2005;83(10):764–773.
- [18] Vashukova ES, GLOTOV AS, FEDOTOV PV, et al. Placental microRNA expression in pregnancies complicated by superimposed preeclampsia on chronic hypertension. *Mol Med Rep*. 2016;14(1):22–32.
- [19] Choi SY, Yun J, Lee O-J, et al. MicroRNA expression profiles in placenta with severe preeclampsia using a PNA-based microarray. *Placenta*. 2013;34(9):799–804.
- [20] Timofeeva AV, Gusar VA, Kan NE, et al. Identification of potential early biomarkers of preeclampsia. *Placenta*. 2018;61:61–71.
- [21] Taganov KD, Boldin MP, Chang K-J, et al. NF-kappaB-dependent induction of microRNA miR-146, an inhibitor targeted to signaling proteins of innate immune responses. *Proc Natl Acad Sci U S A*. 2006;103(33):12481–12486.
- [22] O'Connell RM, Taganov KD, Boldin MP, Cheng G, Baltimore D. MicroRNA-155 is induced during the macrophage inflammatory response. *Proc Natl Acad Sci U S A*. 2007;104(5):1604–1609.
- [23] Sheedy FJ, Palsson-McDermott E, Hennessy EJ, et al. Negative regulation of TLR4 via targeting of the proinflammatory tumor suppressor PDCD4 by the microRNA miR-21. *Nat Immunol*. 2010;11(2):141–147.
- [24] Dai Y, Diao Z, Sun H, et al. MicroRNA-155 is involved in the remodelling of human-trophoblast-derived HTR-8/SVneo cells induced by lipopolysaccharides. *Hum Reprod*. 2011;26(7):1882–1891.
- [25] Kim S, Lee K-S, Choi S, et al. NF-kappaB-responsive miRNA-31-5p elicits endothelial dysfunction associated with preeclampsia via down-regulation of endothelial nitric-oxide synthase. *J Biol Chem*. 2018;293(49):18989–19000.
- [26] Rizzo G, Capponi A, Cavicchioni O, Vendola M, Arduini D. Placental vascularization measured by three-dimensional power Doppler ultrasound at 11 to 13 + 6 weeks' gestation in normal and aneuploid fetuses. *Ultrasound Obstet Gynecol*. 2007;30(3):259–262.
- [27] Mihiu CM, Drugan T, Mihiu D. Contribution of 3D power Doppler ultrasound to the evaluation of placental circulation in normal pregnancies and pregnancies complicated by preeclampsia. *J Perinat Med*. 2012;40(4):359–364.
- [28] Livak KJ, Schmittgen TD. Analysis of relative gene expression data using real-time quantitative PCR and the 2(-Delta Delta C(T)) Method. *Methods*. 2001;25(4):402–408.
- [29] Takacs P, Kauma SW, Sholley MM, et al. Increased circulating lipid peroxides in severe preeclampsia activate NF-kappaB and upregulate ICAM-1 in vascular endothelial cells. *Faseb J*. 2001;15(2):279–281.
- [30] Niu ZR, Han T, Sun X-L, et al. MicroRNA-30a-3p is overexpressed in the placentas of patients with preeclampsia and affects trophoblast invasion and apoptosis by its effects on IGF-1. *Am J Obstet Gynecol*. 2018;218(2):249 e1–249 e12.
- [31] Gao T, Deng M, Wang Q. MiRNA-320a inhibits trophoblast cell invasion by targeting estrogen-related receptor-gamma. *J Obstet Gynaecol Res*. 2018;44(4):756–763.
- [32] Xie N, Jia Z, Li L. miR320a upregulation contributes to the development of preeclampsia by inhibiting the growth and invasion of trophoblast cells by targeting interleukin 4. *Mol Med Rep*. 2019;20(4):3256–3264.
- [33] Brkic J, Dunk C, O'Brien J, et al. MicroRNA-218-5p promotes endovascular trophoblast differentiation and spiral artery remodeling. *Mol Ther*. 2018;26(9):2189–2205.
- [34] Aban M, Cinel L, Arslan M, et al. Expression of nuclear factor-kappa B and placental apoptosis in pregnancies complicated with intrauterine growth restriction and preeclampsia: an immunohistochemical study. *Tohoku J Exp Med*. 2004;204(3):195–202.
- [35] Xue P, Fan W, Diao Z, Li Y, Kong C, Dai X, Peng Y, Chen L, Wang H, Hu Y, et al. Up-regulation of PTEN via LPS/AP-1/NF-kappaB pathway inhibits trophoblast invasion contributing to preeclampsia. *Mol Immunol*. 2020;118:182–190.
- [36] Silva Carmona A, Mendieta Zeron H. NF-kappaBeta and SOD expression in preeclamptic placentas. *Turk J Med Sci*. 2016;46(3):783–788.
- [37] Luppi P, Tse H, Lain KY, Markovic N, Piganelli JD, DeLoia JA. Preeclampsia activates circulating immune cells with engagement of the NF-kappaB pathway. *Am J Reprod Immunol*. 2006;56(2):135–144.
- [38] Shah TJ, Walsh SW. Activation of NF-kappaB and expression of COX-2 in association with neutrophil infiltration in systemic vascular tissue of women with preeclampsia. *Am J Obstet Gynecol*. 2007;196(1):48 e1–8.